Towards long lasting zirconia-based composites for dental implants: Transformation induced plasticity and its consequence on ceramic reliability

Helen Reveron [a], Marta Fornabaio [b], Paola Palmero [b], Tobias Fürderer [c], Erik Adolfsson [d], Vanni Lughi [e], Alois Bonifacio [e], Valter Sergo [e], Laura Montanaro [b], Jérôme Chevalier [a,f,*]

[a] Université de Lyon-INSA de Lyon, MATEIS CNRS UMR 5510, 20 Avenue Albert Einstein, F-69621 Villeurbanne Cedex, France
[b] Department of Applied Science and Technology, INSTM R.U. PoliTO, LINCE Lab., Politecnico di Torino, Corso Duca degli Abruzzi, 24, 10129 Torino, Italy
[c] DOCERAM, MOESCHTER GROUP Holding GmbH & Co. KG, Hesslingsweg 65 – 67, 44309 Dortmund, Germany
[d] Ceramic Materials, Swerea IVF AB, 431 53 Mölndal, Sweden
[e] Dept. of Engineering and Architecture, University of Trieste, Via Valerio 6a-34127–Trieste (TS), Italy
[f] Institut Universitaire de France, 103 bd Saint-Michel, 75005 Paris, France

ARTICLE INFO

Accepted 16 November 2016

Keywords:
Zirconia
Alumina
Composite
Mechanical properties
Plasticity

ABSTRACT

Zirconia-based composites were developed through an innovative processing route able to tune compositional and microstructural features very precisely. Fully-dense ceria-stabilized zirconia ceramics (84 vol % Ce-TZP) containing equiaxed alumina (8 vol%Al_2O_3) and elongated strontium hexa-aluminate (8 vol% $SrAl_{12}O_{19}$) second phases were obtained by conventional sintering. This work deals with the effect of the zirconia stabilization degree (CeO_2 in the range 10.0–11.5 mol%) on the transformability and mechanical properties of Ce-TZP-Al_2O_3-$SrAl_{12}O_{19}$ materials.

Vickers hardness, biaxial flexural strength and Single-edge V-notched beam tests revealed a strong influence of ceria content on the mechanical properties. Composites with 11.0 mol% CeO_2 or above exhibited the classical behaviour of brittle ceramics, with no apparent plasticity and very low strain to failure. On the contrary, composites with 10.5 mol% CeO_2 or less showed large transformation-induced plasticity and almost no dispersion in strength data.

Materials with 10.5 mol% of ceria showed the highest values in terms of biaxial bending strength (up to 1.1 GPa) and fracture toughness (>10 MPa$\sqrt{m}$). In these ceramics, as zirconia transformation precedes failure, the Weibull modulus was exceptionally high and reached a value of 60, which is in the range typically reported for metals. The results achieved demonstrate the high potential of using these new strong, tough and stable zirconia-based composites in structural biomedical applications.

Statement of Significance

Yttria-stabilized (Y-TZP) zirconia ceramics are increasingly used for developing metal-free restorations and dental implants. Despite their success related to their excellent mechanical resistance, Y-TZP can undergo Low Temperature Degradation which could be responsible for restoration damage or even worst the failure of the implant. Current research is focusing on strategies to improve the LTD resistance of Y-TZP or to develop alternative composites with better stability *in vivo*. In this work the mechanical characterization of a new type of very-stable zirconia-based composites is presented. These materials are composed of ceria-stabilized zirconia (84 vol%Ce-TZP) containing two second phases (α-alumina and strontium hexa-aluminate) and exhibit exceptional strength, toughness and ductility, which may allow the processing of dental implants with a perfect reliability and longer lifetime.

1. Introduction

Unlike traditional ceramics which tend to be hard and brittle, zirconia-based materials can exhibit significant inelastic strain

* Corresponding author at: Université de Lyon-INSA de Lyon, MATEIS CNRS UMR 5510, 20 Avenue Albert Einstein, F-69621 Villeurbanne Cedex, France.
E-mail address: Jerome.chevalier@insa-lyon.fr (J. Chevalier).

[1–3]. Transformation from metastable tetragonal (t) zirconia grains to the monoclinic (m) symmetry leads to a powerful strengthening mechanism that allows zirconia systems to be considered as analogues to some metals [4]. Nevertheless, as this transformation behaviour strongly depends on the composition and microstructure of materials, the development of ductile ceramics for structural applications is still a matter of debate.

In the dental field, there is a growing demand for strong, tough and stable inorganic materials which are able to meet specifications of metal-free restorations and implants. These materials are especially needed in the posterior part of the mouth, where crowns, bridges and abutments are subjected to the highest stresses. They are equally necessary for implants which are always subjected to challenging mechanical conditions [5]. At the present time, dental community focus mainly on yttria-stabilized zirconia (Y-TZP) polycrystalline ceramics for these applications, since traditional glass-ceramics and polycrystalline alumina appear to be reaching their limits. Y-TZP ceramics are considered suitable materials for aesthetic dental restorations and implants due to their toughness and strength properties. Nevertheless, they have their unfortunate Achilles' heel-their propensity to undergo Low Temperature Degradation (LTD) in the presence of water [6–8]. LTD, often referred as *ageing*, has been known for over 20 years, but its effects at ambient temperature were underestimated until the end of 90's when several studies showed that this phenomenon could occur under *in vivo* conditions within time scale the orders of years [9,10]. Therefore, current research is focusing on strategies to avoid LTD of Y-TZP [11–16] and on developing innovative composites with a perfect stability *in vivo* and outstanding mechanical properties which will be able to replace alumina or Y-TZP commonly used in the dental field.

Since 1985, ceria-stabilized zirconia (Ce-TZP) has been extensively studied due to its ability to undergo larger amount of stress-induced phase transformation which in turn leads to higher fracture toughness as compared to Y-TZP [17]. Moreover, there is added safety against ageing for as long as cerium ions keep their tetravalent character after sintering [9,18]. Unfortunately, grain growth which takes place during Ce-TZP sintering leads to a lower mechanical resistance (flexural strength of about 500 MPa for Ce-TZP ceramics as compared to 1 GPa for Y-TZP) [19]. From an aesthetic viewpoint, Ce-TZP ceramics exhibit a yellowish colour which limits their use as frontal teeth restorations. Extensive research has been focused on decreasing the grain size by adding an immiscible second phase to the matrix with the aim of increasing the strength and other mechanical properties of Ce-TZP based ceramics. Reasonably strong and tough nanocomposites based on Ce-TZP were developed through the addition of round-shaped and/or elongated second phases, which can hinder the zirconia grain growth and further improve the toughness. Among the several oxides added to Ce-TZP composites, alumina has certainly been one of the most employed. The first work done on this topic belongs to Sato et al. [20] who in 1989 reported a refinement of zirconia grains (from 3.5 to 1.5 μm) and an increase in hardness, strength and thermal shock resistance of 12Ce-TZP/20wt%-Al_2O_3 intergranular composites (12 mol% CeO_2, zirconia grain size 1.5 μm, alumina grain size 500 nm). Thereafter, several authors developed Ce-TZP/alumina composites characterized by zirconia grains of about 1 μm in size [21–23] and enhanced its strength. In 1998, fracture toughness values of 9.8 MPa$\sqrt{}$m and bending strength of 950 MPa were reported by Nawa et al. [24] on 10Ce-TZP-based composites (10 mol% CeO_2, zirconia grain size 1 μm) containing 30vol% of alumina particles (10–100 nm-sized with few alumina particles located intragranularly). Microstructural and compositional features of these composites were optimized, patented (US 7928028) and a commercial product named NANOZR (Panasonic Electric Works, Japan) has since then been commercialized (fracture toughness of 8.6 MPa$\sqrt{}$m and bending strength of 1290 MPa per the ISO standard 6872). Recently, very high fracture toughness (15 MPa$\sqrt{}$m) and excellent flexural strength (900 MPa) were reported by Apel et al. [25] on 10Ce-TZP/16 vol% $MgAl_2O_4$ composites (zirconia and magnesium spinel grain size of 500 and 300 nm, respectively). With the aim of further improving the toughness via activating mechanisms such as bridging/crack-deflection, the addition of elongated third phases has been proposed. First works dating from 1994 showed the improvement of both toughness and strength on 12Ce-TZP/Al_2O_3 composites containing $SrAl_{12}O_{19}$ and $LaAl_{11}O_{18}$ [26,27] platelets. Since then, only a few authors have developed Ce-TZP composites incorporating elongated phases (e.g. aluminates) but studies are still needed to completely understand the toughening mechanism operating in these complex materials [28–32]. However, if it is well accepted that the presence of second phases in zirconia-based ceramics inevitably plays a role in the efficiency of the phase transformation toughening, the most common composites usually remain brittle (flaw sensitive) and failure occurs before a generalized phase transformation with Weibull moduli never exceeding values of 20 (when reported) [33].

Even though the mechanical properties of Ce-TZP based composites have been enhanced in the last few years, further toughness and strength improvements appear to be within reach if complex microstructures (finer zirconia grains, inter-intragranular second phases with different geometries…) with specific compositions (precise control of stabilizer amount, nature of the second phases…) can be developed. Within the framework of a project called *LongLife* ("Advanced multifunctional zirconia ceramics for long-lasting implants", 7th European Framework Program), a new attractive Ce-TZP based ceramic, with high strength, toughness and stability *in vivo* was developed. The processing strategy was based on the *in-situ* formation of both equiaxed alumina (α-Al_2O_3) and elongated aluminate ($SrAl_{12}O_{19}$) phases in a Ce-TZP matrix containing precise amounts of ceria. Zirconia-based materials (84 vol% ZrO_2/8 vol% Al_2O_3/8 vol% $SrAl_{12}O_{19}$ with ceria in the range 10.0–11.5 mol%) immune to LTD (i.e. stabilized with ceria), with enhanced strength (grains refinement by the addition of immiscible phases) and optimized phase transformation toughening (ceria content precisely adapted) were processed from ceria-stabilized commercial powders which were modified by means of a powder-surface coating method [34]. In the present work, the mechanical properties of these composites are analysed. Vickers hardness, biaxial flexural strength and fracture toughness results are discussed on the basis of the tetragonal to monoclinic zirconia phase transformation, which strongly depended on ceria composition. Mechanical behaviour laws are analysed in terms of the transformation-induced plasticity that takes place before failure.

2. Materials and methods

2.1. Composites

For processing Ce-TZP-based composites [34], a commercial 10 mol% ceria–stabilized zirconia powder (Daiichi Kigenso Kagaku Kogio Co. LTD, Japan, hereinafter referred to as 10Ce-TZP) was dispersed in distilled water. Aluminium, strontium and ammonium cerium nitrates (Sigma-Aldrich) were added to 10Ce-TZP aqueous suspensions as precursors of α-alumina, strontium hexaaluminate and to precisely adjust the ceria content in final materials. The suspension was spray-dried and the resulting powder was thermally treated at 1150 °C for 30 min to obtain a tri-phasic zirconia-alumina-strontium aluminate powder. Granules were then redispersed in water and slip-casted. Finally, as-shaped green-ceramics were sintered at 1450 °C/1 h to reach >99.9% of

the theoretical density (TD). Final densities were evaluated by Archimedes' method and the percentage of the theoretical density calculated. TD of composites were estimated by the rule of mixtures from density values of 6.19, 5.82, 3.99 and 4.02 g/cm^3 for tetragonal and monoclinic ZrO_2, α-Al_2O_3 and $SrAl_{12}O_{19}$, respectively. As discussed in the first part of this work [34], preliminary trials allowed us to focus on composites in which the Al_2O_3 and $SrAl_{12}O_{19}$ contents were both fixed at 8 vol%, since they exhibited the finest microstructures after sintering. Therefore, the composition of materials here examined was 84 vol% ZrO_2/8 vol% Al_2O_3/8 vol% $SrAl_{12}O_{19}$ (hereinafter referred to as ZA_8Sr_8) with four ceria contents ranging from 10.0–11.5 mol%. These materials are referred to as ZA_8Sr_8-Ce10, ZA_8Sr_8-Ce10.5, ZA_8Sr_8-Ce11 and ZA_8Sr_8-Ce11.5, being the first and only one in which no extra cerium was added when modifying the 10Ce-TZP commercial powder. In order to confirm the mechanical behaviour observed in the most promising composition (ZA_8Sr_8-Ce10.5), as-spray-dried and thermal treated granules (1150 °C for 30 min) were cold-isostatically pressed (300 MPa) and sintered at 1450 °C/1 h. 23 samples were thus processed and subjected to biaxial tests. In addition, a benchmark of yttria-stabilized zirconia (3Y-TZP) was also prepared [35] from commercially-available granules (TZ-3YSB-E, Tosoh Corporation, Japan), which were cold-isostatically pressed and sintered at 1450 °C/2 h. Microstructures of ceramics were characterized by means of Scanning Electron Microscopy (SEM-Zeiss SUPRA VP55) and High Resolution Transmission Electron Microscopy (HRTEM-JEOL 2010F). The average grain sizes of zirconia and alumina were estimated from SEM micrographs by means of the linear intercept method using 1.56 as the correction factor [36]. The average length and thickness of strontium aluminate were estimated directly from SEM micrographs without introducing any correction. Approximately 200 grains for each phase were considered. Before and after mechanical tests, samples were submitted to XRD analyses (Philips PW 1710 diffractometer, Cu K_α, 10–70°, step size 0.05°, time for step 5 s) in order to evaluate the content of the monoclinic phase (V_m) through the Toraya's equation [37].

2.2. Mechanical characterization

Vickers hardness (Vickers Testwell FV-700) was measured on surfaces polished down to 1 μm using diamond paste. Three different loads (50, 100, 300 N) were applied for 10 s and the average value of five indentations was considered. Vickers hardness was calculated as per the ASTM E384 standard and converted to SI units (GPa). Diagonal lengths were measured using an optical microscope equipped with Nomarski interference contrast (Zeiss Axiophoto). The distance between the centres of two adjacent indentations was at least 3 times the mean diagonal length. The capability of composites to undergo stress-induced phase transformation or transformability was evaluated by measuring the extent of the transformed area around the Vickers indentations. The average value of five indentations for each load was reported. Young's modulus was measured by Grindo-Sonic test (ASTM C1259-01).

Toughness and strength were estimated following the ISO standard 6872 devoted to ceramic materials in dentistry, as one possible short-term application of the composites here developed could be the fabrication of dental implants.

For toughness measurements, ceramics were machined (CNC DMU60 monoBLOCK®, DMG, Germany) on all sides with diamond grinding tools to a rectangular cross section of (4.0 × 3.0) ± 0.2 mm. The final machining of the tensile surface was performed with a 16 μm diamond grinding tool. The samples were subsequently notched using a diamond charged cutting wheel of 300 μm in thickness. The notches were cut across the 3 mm wide surface perpendicular to the length of the bar and sharpened using a razor blade and 3 μm diamond polishing paste. The final notch depth, in the range of 0.8–1.2 mm, was accurately evaluated by means of optical microscopy (Zeiss, Axiophot). In order to minimize the effect of residual stresses developed during sample preparation, an annealing treatment was applied (1200 °C/30 min).Toughness was measured by the Single Edge V-Notched Beam (SEVNB) method in a four-point bending fixture (universal hydraulic testing machine, Instron 8500, USA). The load was applied to the side which is 4 mm wide at 0.5 mm/min until failure is obtained. Only tests in which the crack started at the bottom of the V-notch and propagated over the bar width were considered valid. Average fracture toughness was estimated from 6 (ZA_8Sr_8-Ce10), 5 (ZA_8Sr_8-Ce10.5; ZA_8Sr_8-Ce11) and 4 (ZA_8Sr_8-Ce11.5) tested-samples.

Piston-on-three balls biaxial bending strength was determined from ten samples of each composition. During the test, discs were subjected to biaxial stresses in their central region and the maximum tensile stress occurred at the centre of the surface opposite to the application of the load (bottom plane of the disc). Samples with a diameter of 12–15 mm were machined on both sides, using cooling, to ensure that opposite faces were flat and did not differ more than 0.05 mm in parallelism. Final machining of tensile surfaces was performed by grinding with a 16 μm diamond tool until a sample thickness of 1.2 ± 0.2 mm was reached (CNC DMU60 monoBLOCK®, DMG, Germany). According to the ISO standard 6872 no annealing treatment was applied. The cross-head speed was set to be at 1 mm/min until failure was achieved. For the most promising composition (ZA_8Sr_8-Ce10.5), a set of 23 samples were tested, allowing for the estimation of the Weibull modulus.

In addition, in order to better characterize the tetragonal to monoclinic phase transformation during loading, a sample of each composition was polished down to 1 μm using diamond paste (only the tensile surface was polished) and submitted to a load-unload test. Starting with 500 MPa, the stress was increased by steps of 100 MPa until failure. Slow-crack propagation was avoided by setting the cross-head speed at 100 MPa/s. Optical microscopy examinations with Nomarski interference contrast were performed at each stage of unloading on surfaces submitted to tensile stress (bottom plane of the disc). Raman maps were collected after the failure on tensile surfaces using an InVia Raman microscope (Renishaw plc, Wotton-under-Edge, UK) equipped with a high-power 785 nm near infrared diode laser (Toptica Photonics AG, Germany) delivering 120 mW of laser power to the sample (x10 objective, N. A. 0.25). Raman data analysis was performed with the R software environment for statistical computing and graphics [38] and with the Fityk software [39] for curve fitting, allowing for mapping of monoclinic/tetragonal phase content and stresses. For each spectrum, the monoclinic volume fraction (%) was calculated from peak areas according to Tabares and Anglada [40] based on Katagari et al. equations, and the residual stress was calculated based on the relative peak positions according to Tomaszewski et al. [41].

3. Results and discussion

3.1. Composite microstructural features

To present an example, Fig. 1 shows SEM and HRTEM images of one of the composites produced by slip-casting and conventional sintering, demonstrating the exceptional fine microstructure of the material, its homogeneity and the presence of three main phases: ceria-stabilized zirconia (*Z*), alumina (A) and strontium hexa-aluminate (S). As discussed in Part I of this work [34], cerium was found only inside zirconia grains. Independently of the ceria content (10.0, 10.5, 11.0 and 11.5 mol% CeO_2), all sintered samples presented practically the same microstructural features, with zirconia grains having an average size of 0.6 ± 0.2 μm (Ce-stabilized ZrO_2), alumina grains of 0.3 ± 0.1 μm (α-Al_2O_3) and strontium

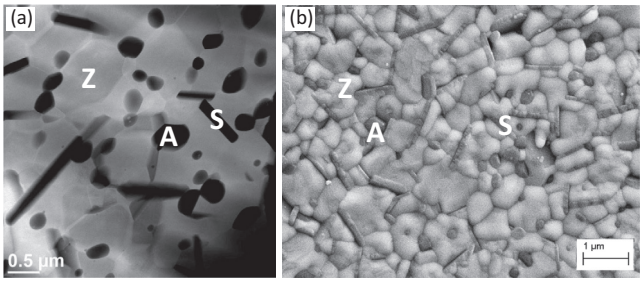

Fig. 1. (a) TEM and (b) SEM images of composites containing 84 vol% Ce-TZP, 8 vol% α-alumina and 8 vol% strontium hexa-aluminate (bright zirconia grains, dark round-shaped α-Al_2O_3 grains and dark elongated $SrAl_{12}O_{19}$ grains are observed).

hexa-aluminate grains with a mean length of 0.6 ± 0.2 µm and aspect ratio of 5 ± 2 ($SrAl_{12}O_{19}$).

All sintered composites reached full densification (>99.9%TD) and exhibited a monoclinic volume fraction <1 vol%. After the grinding step down to 16 µm, monoclinic volume content increased to 15 (ZA_8Sr_8-Ce10), 10 (ZA_8Sr_8-Ce10.5), 3 (ZA_8Sr_8-Ce11) and 6 (ZA_8Sr_8-Ce11.5) vol%. The increase of the monoclinic phase on grinded surfaces as compared to the as-sintered ones can be attributed to the tetragonal to monoclinic phase transformation that occurs under mechanical stresses [42,43]. Nevertheless, in samples mirror-polished down to 1 µm with diamond paste, no monoclinic phase was detected by XRD. Y-TZP zirconia benchmark was also full densified and exhibited zirconia grains of about 0.4 ± 0.2 µm in size.

3.2. Hardness of ZA_8Sr_8-based composites

HV30 (300 N load) hardness for ZA_8Sr_8 composites as a function of ceria amount are reported in Fig. 2. Hardness fluctuated in the range of 9.8–10.6 GPa and, with the exception of ZA_8Sr_8-Ce10.5 composite, increased with ceria contents. Despite the addition of a softer phase (strontium hexa-aluminate) as compared to magnesia spinel or alumina, hardness values were in the range typically reported in Ce-TZP composites containing alumina, strontium or magnesium-based second phases (9–12 GPa) [24–26]. Given that all the processed composites presented almost the same microstructural features and density [34], the increase in hardness can be attributed to the stabilization degree of zirconia by considering the tetragonal to monoclinic phase transformation that took

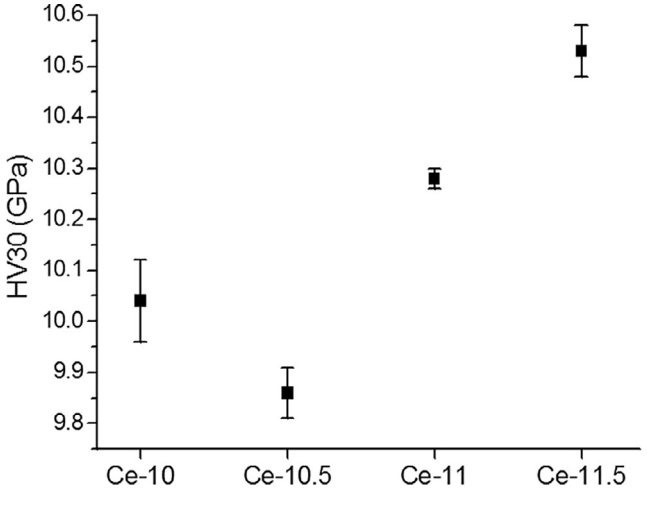

Fig. 2. Vickers hardness of ZA_8Sr_8 composites at 300 N of load as a function of the ceria amount. The errors bars represent the standard deviation of five indentations.

place under the indenter. As reported by Hannink and Swain [44], partially-stabilized zirconia hardness decreases with the increase of the size of the plastic deformation zone formed around the indentation imprint.

More precise characterization of the transformability of ZA_8Sr_8-based composites is given in Fig. 3. After Vickers tests, the brighter zone around the indentation imprint is associated to the part of the material in which the tetragonal to monoclinic transformation of zirconia occurred, resulting in a volume increase (4–5 vol%). As expected, the amount of phase transformation was the largest for higher applied loads, regardless of the ceria amount. The size of the transformed zone corroborates the higher transformability of zirconia in less-stabilized ZA_8Sr_8-Ce10 and ZA_8Sr_8-Ce10.5 composites with respect to ZA_8Sr_8-Ce11 and ZA_8Sr_8-Ce11.5. Additionally, transformed areas exhibited different morphologies. A large number of transformation branches which propagate radially from the middle of the imprints were observed on ZA_8Sr_8-Ce10 and ZA_8Sr_8-Ce10.5 surfaces, associated to the autocatalytic nature of the transformation. As reported by Reyes et al. [45], autocatalysis initiates by a nucleation event that, once realized, can stimulate further transformation over an extended region. On the contrary, smaller and round-shaped transformed zones with less developed branches were observed on ZA_8Sr_8-Ce11 and ZA_8Sr_8-Ce11.5, where the stability of zirconia grains was increased. In all examined samples, no cracking from the Vickers indenter tip was produced once loads of 50 and 100 N were applied. Only few and very short cracks appeared in certain samples tested at 300 N, but their lengths were insufficient for the application of indentation techniques to determine fracture toughness. Remarkably, this behaviour qualitatively indicates the very high flaw tolerance of all investigated composites. In the case of the 3Y-TZP benchmark, the transformation zone was hardly visible in surfaces subjected to 300 N and long cracks were developed from the tip, corroborating a lower flaw tolerance.

3.3. Load-displacement behaviour

The effect of ceria content on the biaxial load-displacement curves is presented in Fig. 4. Here, the vertical axis represents the applied load while the horizontal one represents the displacement measured on the 3-balls side surface by means of a linear variable differential transformer (LVDT sensor). Optical microscopy characterization using Nomarski contrast is also displayed in these figures for applied stresses of 500 MPa and after failure (maximum stresses of 680, 1100, 772 and 756 MPa for 10.0, 10.5, 11.0 and 11.5 mol% CeO_2, respectively). Nomarski interference enables the easy recognition of the branches of the monoclinic phase associated to zirconia phase transformation. Two distinct behaviours were identified. The first, in composites with ceria contents of 11.0 mol% or above, was the standard ceramic-like behaviour without a measurable yield stress and a linear load-displacement curve. As expected, optical microscopy characterization revealed a very limited tetragonal to monoclinic transformation zone around cracks, corroborating their lower transformability. For both compositions (11.0 and 11.5 mol% Ce), no transformed zone was observed after an applied stress of 500 MPa and the critical transformation stress (σ^c_{t-m}) was about 600 MPa (stress from which transformation was observed over the sample surface). As for the second, composites with a ceria content of 10.5 mol% or less exhibited a very peculiar behaviour, generally observed in ductile metals. In particular, composites with 10.0 mol% Ce showed a pronounced plasticity and a strain to failure estimated at 0.5% based on the assumption of linear-elastic behaviour. All load-unload curves ran parallel even for large strain, demonstrating that plasticity occurs without damage, as in the case of ductile materials (load-unload cycles revealed significant permanent deforma-

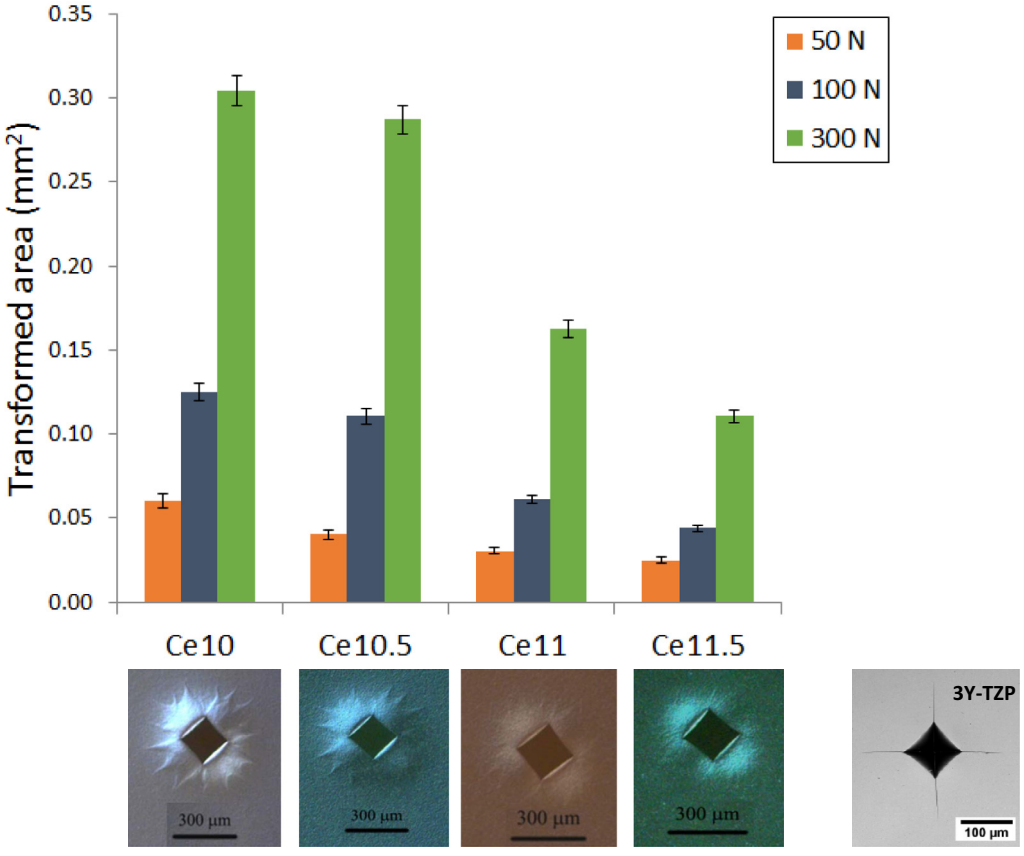

Fig. 3. Transformed area on ZA_8Sr_8 composites after Vickers tests at different loads and 3Y-TZP benchmark (optical images were recorded at 300 N). The error bars represent the standard deviation of five area measurements for each applied load.

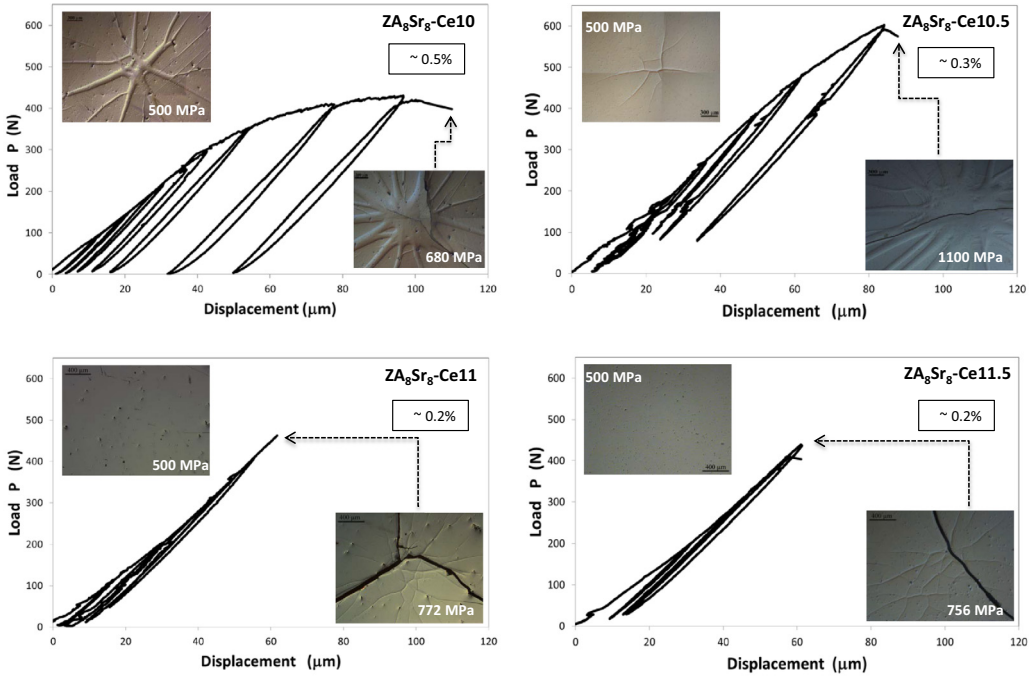

Fig. 4. Effect of ceria content on the load-displacement behaviour of various Ce-TZP composites. Optical characterization of tensile surfaces after 500 MPa and failure is also displayed.

tion, while the Young's modulus was preserved). A yield stress of 300 MPa and 450 MPa can be estimated for 10.0 and 10.5 mol% Ce respectively, which should correspond to the onset of the zirconia phase transformation. For both compositions (10.0 and

10.5 mol% Ce), monoclinic to tetragonal transformation started well before crack propagation and expanded when increasing applied stress, as shown in the insets of the Fig. 4.

Our observations showing a metal-like behaviour in these composites are not new. Ce-TZP based ceramic plasticity has been reported in previous works [1–3,45]. Nevertheless, the significance of our results lies in the fact that, because of the particular microstructure and composition of new developed composites [34], plasticity is observed at higher stresses in this instance. It is clear from Fig. 4 that yield stress and strength reached a maximum for a ceria content of 10.5 mol% (optimized critical transformation stress). The capability to undergo plastic deformation is here driven by the phase transformation and represents a great advantage for many applications, as compared to standard brittle ceramics such as alumina, 3Y-TZP or even all biomedical grade ceramics developed so far.

Fig. 5 shows the superposition of an optical microscopy image (Nomarski contrast) and a monoclinic/tetragonal Raman map obtained by analysing the tensile surface of a biaxial tested disc. The stress Raman map along the transformed zone is also displayed. Monoclinic phase regions observed in the Raman map closely reproduced the branches revealed via Nomarski contrast, corroborating the fact that they correspond to zones in which the tetragonal to monoclinic transformation has taken place. A maximum monoclinic content of 70vol% was estimated inside the transformed zone, while on the areas in between and around branches, no monoclinic phase was detected. Because of the transformation of zirconia, compressive stresses as high as 1GPa were created. These compressive stresses contribute to shield tensile stresses applied during bending. It is worth noting that even if the depth analysed by Raman was a few times larger than that probed by XRD, the same findings were achieved. Moreover, XRD analyses performed on fractured surfaces of samples submitted to SEVNB tests revealed a monoclinic phase content in the range of 70–55 vol% when passing from 10.0–11.5 mol% of ceria (68vol% in ZA_8Sr_8-Ce10.5). All of these results showed that the entirety of investigated compositions possessed relatively high fracture toughness and transformability. In contrast with this behaviour, the XRD content of monoclinic phase reached only 3 vol% in 3Y-TZP fractured surfaces, as expected given its moderate fracture toughness.

3.4. Fracture toughness and biaxial flexural strength

Fig. 6 presents the fracture toughness and biaxial flexural strength for different compositions and the probability of failure and properties for the optimal composition. ZA_8Sr_8-based materials were characterized by fracture toughness in the range of 8.2–10.2 $MPa\sqrt{m}$. The toughness increased when the ceria content was decreased and was always higher than in 3Y-TZP (6.6 $MPa\sqrt{m}$). Nevertheless, toughness determined in ZA_8Sr_8-Ce10 sample was underestimated, since tested samples remained unbroken even at the maximum load applied by the testing machine (1KN). This fact highlights once more the extraordinary "ductile-like" behaviour observed in such very transformable material, which hampers correct K_{IC} measurements by the SENVB method. Similarly, toughness for ZA_8Sr_8-Ce10.5 was also underestimated given that half of the tested specimens were not broken. Thus, for these two compositions fracture toughness higher than 10.2 $MPa\sqrt{m}$ can be reasonably assumed but it is necessary to con-

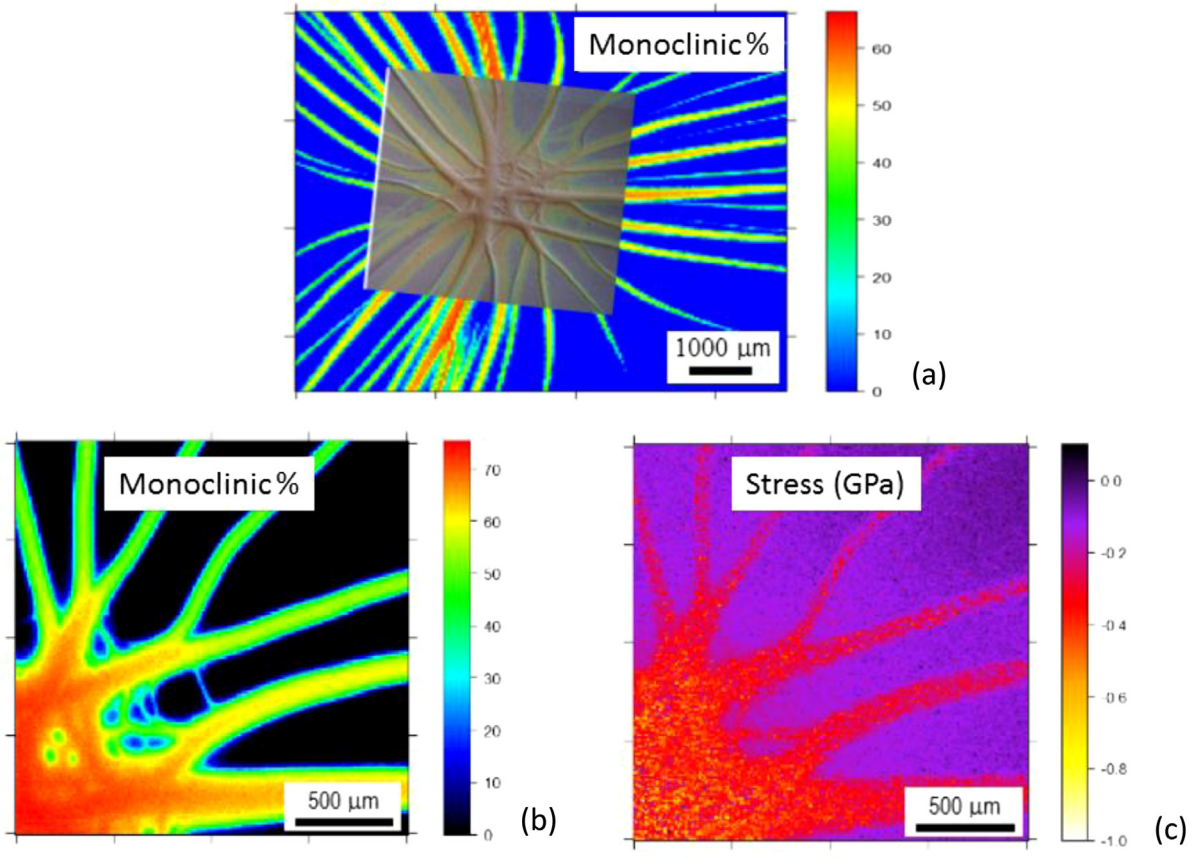

Fig. 5. Monoclinic phase transformation (vol%) on ZA_8Sr_8-Ce10.5 after biaxial test (a) Nomarski optical microscopy superposed to Raman map, (b) Monoclinic content in the transformed zone, (c) Compressive stresses associated to the phase transformation.

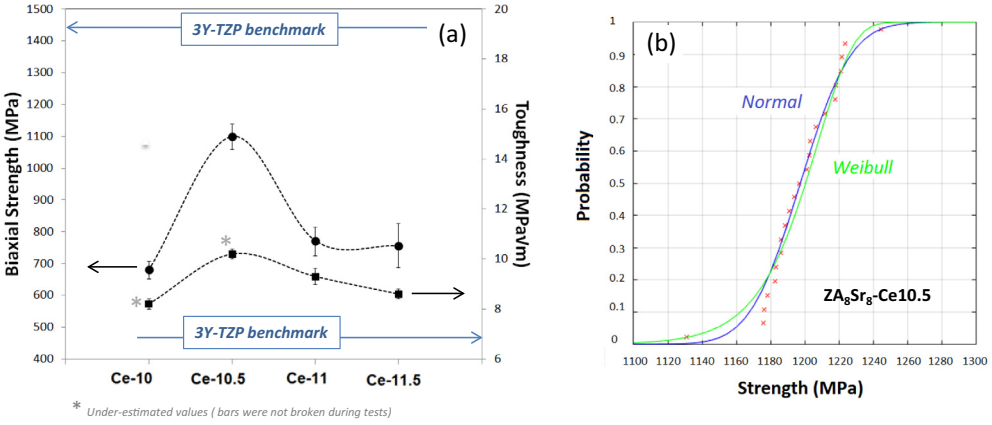

Property ZA_8Sr_8-Ce10.5	Value (c)
Bending strengh	1100 ± 39 MPa (slip-casting, N=10) 1197 ± 23 MPa (cold-isostatic pressing, N=23)
Fracture toughness	10.2± 0.2 MPa√m
Weibull modulus (m)	60
Young modulus	216 GPa
LTD	Not observed

Fig. 6. (a) Biaxial flexural strength and fracture toughness for different slip-casted and sintered ceramics. The error bars represent the standard deviation of ten (strength) or three (toughness) measurements (b) Weibull and normal probability plots of the biaxial flexural strength of ZA_8Sr_8-Ce10.5 samples (N = 23) cold-isostatically pressed and sintered (c) Properties of the optimal composition.

duct further analyses with other methods (e.g. double torsion or compact tension tests) to try to establish the real fracture toughness. Nowadays, our findings certainly corroborate the strong R-curve behaviour of composites developed in this work, as reported by El Attaoui et al. [19] in 10-CeTZP ceramics. Independent of the ceria amount, the very high fracture toughness observed in ZA_8Sr_8-based composites is related to the excellent transformability of zirconia grains and not to a surface residual stresses effect, since all specimens subjected to SENVB tests were annealed.

ZA_8Sr_8-based materials exhibited a biaxial flexural strength in the range of 680–1100 MPa (±20–70 MPa), depending on the ceria amount they contained. Such high mechanical resistance as compared to pure Ce-TZP monolithic ceramics [17] corroborates the positive effect of refining zirconia grains (by adding Al_2O_3 and $SrAl_{12}O_{19}$ second phases) and of controlling the ceria content. As expected and in agreement with available literature, 3Y-TZP benchmark ceramics showed a higher biaxial flexural strength (1447 MPa) but also the highest standard deviation (±167 MPa). The variability of the strength is attributed to the flaw-sensitivity or brittleness of Y-TZP [46].

As proposed by Swain et al. [47] and reported in other studies dealing with monolithic Ce-TZP [17,24], the limitation of the strength in this type of zirconia-based materials is governed by the critical stress necessary to induce the tetragonal to monoclinic zirconia phase transformation. As microstructural features are almost identical in samples containing different ceria amounts, the strength variability is attributed to the different degree of zirconia stabilization. In less-stabilized samples (containing 10.0 and 10.5 mol% ceria), zirconia transformation starts before crack propagation and the strength depends on the critical transformation strength (σ^c_{t-m}). For higher ceria contents (11.0 and 11.5 mol% ceria), as zirconia becomes more stable, the transformation is hindered and occurs only when a crack propagates from a pre-existing processing flaw. In this instance, the strength is limited by the size of flaws as in the case of classical "brittle" ceramics. The strength reaches therefore a maximum for specific conditions of composition and processing. As shown in Fig. 6(a), the strength increased with ceria content up to 10.5 mol%, then decreased for higher ceria amounts.

To enter into details, strength for high ceria content is given by the classical Griffith's equation:

$$\sigma_f = \frac{K_{IC}}{Y\sqrt{c}} \tag{1}$$

where σ_f is the strength for brittle failure, K_{IC} the toughness, Y a geometrical factor and c the size of the most critical flaw. In the early 80's, McMeeking and Evans [48] described the mechanics of phase transformation in zirconia ceramics and the relation between the amount of phase transformation developed at the crack tip which tends to limit crack tip stresses and toughness. The reader can refer to this paper for a deeper analysis. The real stress intensity factor at the crack-tip K_{Itip} is lower than that applied by the external forces K_I because the stress-induced phase transformation leads to a shielding K_{Ish} of the applied stress intensity factor, as per the following:

$$K_{Itip} = K_I - K_{Ish} \tag{2}$$

Increasing the applied stress intensity factor leads to a larger transformation zone and thus to a larger shielding effect which is proportional to the applied K_I:

$$K_{Ish} = C_{sh}\frac{K_I}{\sigma^c_{t-m}} \tag{3}$$

where σ^c_{t-m} is the critical stress leading to t-m phase transformation and C_{sh} the proportionality constant which depends on the Young's modulus (E), the volume fraction of transformable particles (V_f; here for example 84 vol%), the volume expansion related to the t-

m transformation (e^T) and the Poisson ratio (ν), via the following equation:

$$C_{sh} = \frac{0.214 E V_f e^T (1+\nu)\sqrt{3}}{(1-\nu)12\pi} \quad (4)$$

By substituting Eq. (3) into (2), the shielding associated to the phase transformation can hence be related to the critical transformation stress σ^c_{t-m}:

$$K_{tip} = K_I \left(1 - \frac{C_{sh}}{\sigma^c_{t-m}}\right) \quad (5)$$

If $K_{IC(0)}$ is the initial toughness of the material without phase transformation, the toughness K_{IC} can be written as:

$$K_{IC} = K_{IC(0)} \left(1 + \frac{C_{sh}}{\sigma^c_{t-m}}\right) \quad (6)$$

Substituting Eq. (6) into (1) provides an evolution of strength versus the critical stress for transformation in the form:

$$\sigma_f = \frac{K_{IC(0)} \left(1 + \frac{C_{sh}}{\sigma^c_{t-m}}\right)}{Y\sqrt{c}} \quad (7)$$

Eq. (7) indicates that strength increases when the critical stress for transformation σ^c_{t-m} decreases (i.e. when the stabilizer content decreases). This is in agreement with the experimental results observed for ceria content exceeding 10.5 mol%. Below this value, the maximum stress which can be withstood by the material no longer follows Eq. (7) and the maximum stress is directly related to the apparition of transformation bands on the tensile side of the specimen. The strength becomes transformation-limited, as previously discussed. Transformation stress can be in this case considered as a yield stress for materials like metals. Hence, the evolution of strength versus the critical stress for transformation is written in the form:

$$\sigma_f = \alpha \sigma^c_{t-m} \quad (8)$$

where α is lesser than 1 and considered to be the same for all compositions. For compositions with the highest degree of transformability (ceria content below 10.5 mol%), strength is no longer flaw-size dependent but rather it increases with σ^c_{t-m} (thus with the amount of ceria).

The optimum stress to failure is obtained for a specific transformation stress (i.e. specific ceria content), when Eq. (7) equals Eq. (8), i.e. when σ^c_{t-m} satisfies:

$$\alpha \sigma^c_{t-m} = \frac{K_{IC(0)} \left(1 + \frac{C_{sh}}{\sigma^c_{t-m}}\right)}{Y\sqrt{c}} \quad (9)$$

A very fine-tuning of the compositional features, made possible by the nano-powder engineering approach developed [34] and a decrease in the size of processing flaws is therefore a prerequisite to obtain the optimal strength on these zirconia-based materials.

Having high strength and toughness is important, as it is for the composite with a ceria content of 10.5 mol% exhibiting $\sigma_f \sim 1.1$ GPa and $K_{IC} \geqslant 10$ MPa$\sqrt{m}$. Such values are among the best reported so far for ceramic materials and can compete with those of metals. The critical flaw size in ZA_8Sr_8-Ce10.5 composite estimated by the Griffith's equation [49] was about 100 μm, further demonstrating the extraordinary flaw-tolerant nature of this material.

Another critical issue when considering ceramics for structural applications is their strength distribution. Strength reliability of ceramics is generally low and is characterized by the Weibull strength distribution, whereas yield and failure stresses of metals exhibit low scatter and are modeled by a normal distribution. The large scatter in the strength of ceramic materials (low Weibull modulus) is linked to their sensitivity to pre-existing flaws since failure starts from small defects existing in the material. The scatter of strength, therefore, is caused by the scatter of the flaw size. Fig. 6(b) compiles the experimental biaxial strength distribution measured on 23 samples of the composite with the optimal composition (ZA_8Sr_8-Ce10.5) fitted by a Weibull and a normal distributions. Characteristic strength values are exceptionally high, as anticipated by the load-unload tests and biaxial tests described above (respectively $\sigma_0 = 1205$ MPa and $\sigma_{fmean} = 1197$ MPa). Of even greater importance, a Weibull modulus of $m = 60$ and a standard deviation of 23 MPa were obtained. Such a high Weibull modulus indicates that the composite exhibits almost no dispersion in strength (the dispersion in strength values being even possibly attributed to the variation in testing conditions from one sample to another rather than to the material itself). In other words, the material behaves more like a metal, with a strength limited here by the yield stress attributed to the tetragonal to monoclinic transformation. The implication of these results are extremely important, as they indicate that such composites are flaw tolerant and can be designed in a safer way than current ceramics. Lastly, the best probability fit is obtained by using a normal strength distribution. All these results corroborate with the previous findings that in the optimized composite, the tetragonal to monoclinic transformation precedes failure, given the material quasi-insensibility to the pre-existing defects or flaws. The predictive nature of the strength, associated with the "metal-like" behaviour characterizing these composites, should open the doors of new opportunities to these ceramics.

In Fig. 6(c), the principal properties of the most promising composition are summarized. As compared to the 3Y-TZP benchmark, ZA_8Sr_8-Ce10.5 composite showed higher toughness, stress-induced transformability and ageing resistance, in spite of its lower flexural strength. This composite remained stable after 50 h of ageing test [34] i.e. about 150–200 years *in vivo*. Promising results in terms of bacterial adhesion were also reported by Karygianni et al. [50] further supporting its employment in the biomedical field.

To summarize, in composites here developed, the well-dispersed alumina particles exert an effective pinning on zirconia grain boundaries, making it possible to enhance the critical stress that induces the t-m transformation of Ce-stabilized zirconia. The strontium hexa-aluminate elongated grains could also contribute to enhancing the mechanical properties, especially the resistance to crack-propagation, but further characterization is required to clarify their role (e.g. bridging/crack-deflection mechanisms [26,51] or trigger for phase transformation). Simultaneously, the efficiency of the phase transformation toughening mechanism is preserved by carefully tailoring the ceria content in the composites. In composites containing 10.5 mol% of ceria, the tetragonal to monoclinic transformation took place well before crack propagation, demonstrating that the strength is driven by the transformation with a critical stress not far from 500 MPa. By decreasing the ceria content down to 10.0 mol%, toughness is expected to increase due to a lower stabilization of zirconia but the strength is here limited by the low critical transformation stress (<300 MPa). In contrast, if the ceria content is increased to 11.0 and 11.5 mol%, the transformation toughening is limited by the higher critical transformation stress (close to 600 MPa) and both toughness and strength decreased. In order to better asses the lifetime of these materials in the oral environment, further mechanical characterization conducted in water or physiological fluids (such as strength, toughness, static and cyclic fatigue, etc) is needed.

4. Conclusions

This work discusses the mechanical properties of novel multi-phasic zirconia-based composites having the following composition: 84 vol% Ce-TZP-8 vol% Al_2O_3-8 vol% $SrAl_{12}O_{19}$ and developed by an innovative synthesis process described in Part I of this work. By fine tuning the precise ceria amount inside the zirconia grains (in the range of 10.0–11.5 mol%), four composites differing only in the zirconia stabilization degree were prepared. Vickers hardness, biaxial flexural strength and Single-edge V-notched beam tests revealed a strong relationship between the amount of stabilizing oxide present and the corresponding mechanical response. As assessed by optical microscopy, XRD and Raman spectroscopy, all investigated materials showed relatively high transformability: the monoclinic volume fraction generated by this transformation ranged between 70–55 vol% at the fractured surfaces.

Materials containing 10.5 mol% of ceria inside zirconia grains showed excellent ageing resistance (stability *in vivo* estimated > 150 years) and the best combination of strength (>1 GPa) and toughness (>10 $MPa\sqrt{m}$) which exceed the requirements for the development of dental implants. The fact that transformation occurs well before failure leads to an extraordinary high flaw tolerance which is reflected by a Weibull modulus never before reported for a ceramic (m = 60). The excellent mechanical properties obtained in ZA_8Sr_8-Ce10.5 composites are attributed to the refinement of the microstructure achieved by well-dispersing second phases inside the matrix and by the simultaneous fine-tuned adjusting of the zirconia stabilization degree. The development of these new strong, tough and stable zirconia-based composites enables them to be considered as very promising candidates for structural biomedical applications, for example in dentistry. The predictive nature of their strength, associated with a "metal-like" behaviour, should assure new opportunities for these ceramics in previously unthinkable applications.

Acknowledgement

The research leading up to these results was undertaken in the framework of the *LongLife* project (www.longlife-project.eu) funded by the European Community's Seventh Framework Programme (FP7/2007-2013) under the grant agreement n° 280741.

The authors would like to acknowledge the CLYM team (Centre Lyonnais de Microscopie-http://www.clym.fr) for their contribution in conducting the HRTEM experiments.

References

[1] G. Grathwohl, T. Liu, Crack resistance and fatigue of transforming ceramics: II, CeO_2-stabilized tetragonal ZrO_2, J. Am. Ceram. Soc. 74 (1991) 3028–3034.
[2] G.A. Gogotsi, V.P. Zavada, M.V. Swain, Mechanical property characterization of a 9 mol% Ce-TZP ceramic material-I. Flexural response, J. Eur. Ceram. Soc. 15 (1995) 1185–1192.
[3] G. Rauchs, T. Fett, D. Munz, R. Oberacker, Tetragonal-to-monoclinic phase transformation in CeO_2-stabilised zirconia under uniaxial loading, J. Eur. Ceram. Soc. 21 (2001) 2229–2241.
[4] R.C. Garvie, R.H. Hannink, R.T. Pascoe, Ceramic steel?, Nature 258 (1975) 703–704
[5] J. Geng, K.B.C. Tan, G. Liu, Application of finite element analysis in implant dentistry: a review of the literature, J. Prosthet. Dent. 85 (2001) 585–598.
[6] K. Kobashi, H. Kuwajima, T. Masaki, Phase change and mechanical properties of ZrO_2-Y_2O_3 solid electrolyte after ageing, Solid State Ionics 3–4 (1981) 489–493.
[7] T. Sato, M. Shimada, Transformation of yttria-doped tetragonal ZrO_2 polycrystals by annealing in water, J. Am. Ceram. Soc. 68 (1985). 356-356.
[8] F.F. Lange, G.L. Dunlop, B.I. Davis, Degradation during aging of transformation-toughened ZrO_2-Y_2O_3 materials at 250 °C, J. Am. Ceram. Soc. 69 (1986) 237–240.
[9] M.J. Lance, E.M. Vogel, L.A. Reith, W.R. Cannon, Low-temperature aging of zirconia ferrules for optical connectors, J. Am. Ceram. Soc. 84 (2001) 2731–2733.
[10] J. Chevalier, L. Gremillard, Ceramics for medical applications: a picture for the next 20 years, J. Eur. Ceram. Soc. 29 (2009) 1245–1255.
[11] I.M. Ross, W.M. Rainforth, D.W. McComb, A.J. Scott, R. Brydson, The role of trace additions of alumina to yttria-tetragonal zirconia polycrystals (Y-TZP), Scripta Mater. 45 (2001) 653–660.
[12] F.F. Lange, Transformation toughening I. Size effects associated with the thermodynamics of constrained transformations, J. Mater. Sci. 1 (1982) 225–234.
[13] L. Hallmann, The influence of grain size on low-temperature degradation of dental zirconia, J. Biomed. Mater. Res. B Appl. Biomater. 100 (2012) 447–456.
[14] F. Zhang, K. Vanmeensel, M. Inokoshi, M. Batuk, J. Hadermann, B. Van Meerbeek, I. Naert, J. Vleugelsa, 3Y-TZP ceramics with improved hydrothermal degradation resistance and fracture toughness, J. Eur. Ceram. Soc. 34 (2014) 2453–2463.
[15] F. Zhang, K. Vanmeensel, M. Batuk, J. Hadermann, M. Inokoshi, B. Van Meerbeek, I. Naert, J. Vleugels, Highly-translucent, strong and aging-resistant 3Y-TZP ceramics for dental restoration by grain boundary segregation, Acta Biomater. 16 (2015) 215–222.
[16] I. Tredicia, M. Sebastiani, F. Massimi, E. Bemporad, A. Resmini, G. Merlati, U. Anselmi-Tamburini, Low temperature degradation resistant nanostructured yttria-stabilized zirconia for dental applications, Ceram. Int. 42 (2016) 8190–8197.
[17] K. Tsukuma, M. Shimada, Strength, fracture toughness and Vickers hardness of CeO_2-stabilized tetragonal ZrO_2 polycrystals (Ce-TZP), J. Mater. Sci. 20 (1985) 1178–1184.
[18] V. Lughi, V. Sergo, Low temperature degradation -aging- of zirconia: a critical review of the relevant aspects in dentistry, Dent. Mater. 26 (2010) 807–820.
[19] H. El Attaoui, M. Saâdaoui, J. Chevalier, G. Fantozzi, Static and cyclic crack propagation in Ce-TZP ceramics with different amounts of transformation toughening, J. Eur. Ceram. Soc. 27 (2007) 483–486.
[20] T. Sato, T. Endo, M. Shimada, Postsintering hot isostatic pressing of ceria-doped tetragonal zirconia/alumina composites in an argon-oxygen gas atmosphere, J. Am. Ceram. Soc. 72 (1989) 761–764.
[21] J.F. Tsai, C.S. Yu, D.K. Shetty, Fatigue crack propagation in ceria-partially-stabilized zirconia (Ce-TZP)-alumina composites, J. Am. Ceram. Soc. 73 (1990) 2292–3001.
[22] C.S. Yu, D.K. Shetty, M.C. Shaw, D.B. Marshall, Transformation zone shape effects on crack shielding in ceria-partially-stabilized zirconia (Ce-TZP)-alumina composites, J. Am. Ceram. Soc. 75 (1992) 2991–2994.
[23] H.K. Schmid, R. Pennefather, S. Meriani, C. Schmid, Redistribution of Ce and La during processing of Ce(La)-TZP/Al_2O_3 composites, J. Eur. Ceram. Soc. 72 (1992) 761–764.
[24] M. Nawa, S. Nakamoto, T. Sekino, K. Niihara, Tough and strong Ce-TZP/Alumina nanocomposites doped with Titania, Ceram. Int. 10 (1998) 381–392.
[25] E. Apel, C. Ritzberger, N. Courtois, H. Reveron, J. Chevalier, M. Schweiger, F. Rothbrust, V.M. Rheinberger, W. Höland, Introduction to a tough, strong and stable Ce-TZP/$MgAl_2O_4$ composite for biomedical applications, J. Eur. Ceram. Soc. 32 (2012) 2697–2703.
[26] R.A. Cutler, J.M. Lindemann, J.H. Ulvensøen, H.I. Lange, Damage-resistant SrO-doped Ce-TZP/Al_20_3 composites, Mater. Des. 15 (1994) 123–133.
[27] M. Miura, H. Hongoh, T. Yogo, S. Hirano, T. Fujll, Formation of plate-like lanthanum-β-aluminate crystal in Ce-TZP matrix, J. Mater. Sci. 29 (1994) 262–268.
[28] S. Maschio, G. Pezzotti, O. Sbaizero, Effect of $LaNbO_4$ addition on the mechanical properties of ceria-tetragonal zirconia polycrystal matrices, J. Eur. Ceram. Soc. 18 (1998) 1779–1785.
[29] S. Ori, T. Kojima, T. Hara, N. Uekawa, K. Kakegawa, Fabrication of Ce-TZP/β-hexaaluminate composites using amorphous precursor of the second phase, J. Ceram. Soc. Jpn. 120 (2012) 111–115.
[30] M. Miura, H. Hongoh, T. Yogo, S. Hirano, T. Fujll, Formation of plate-like lanthanum-β-aluminate crystal in Ce-TZP matrix, J. Mater. Sci. 29 (1994) 262–268.
[31] T. Yamaguchi, W. Sakamoto, T. Yogo, T. Fujii, S. Hirano, In situ formation of Ce-TZP/Ba-hexaaluminate composites, J. Ceram. Soc. Jpn. 107 (1999) 814–916.
[32] F. Kern, A comparison of microstructure and mechanical properties of 12Ce-TZP reinforced with alumina and in situ formed strontium- or lanthanum-hexaaluminate precipitates, J. Eur. Ceram. Soc. 34 (2014) 413–423.
[33] M. Lambrigger, Evaluation of Weibull master curves of zirconia ceramics and zirconia/alumina composites, J. Mater. Sci. Lett. 16 (1997) 924–926.
[34] P. Palmero, M. Fornabaio, L. Montanaro, H. Reveron, J. Chevalier, Towards long lasting zirconia-based composites for dental implants. Part I: Innovative synthesis, microstructural characterization and in vitro stability, Biomaterials 50 (2015) 38–46.
[35] I. Denry, J.A. Holloway, Ceramics for dental applications: a review, Materials 3 (2010) 351–368.
[36] M. Mendelson, Average grain size in polycrystalline ceramics, J. Am. Ceram. Soc. 52 (1969) 443–446.
[37] H. Toraya, M. Yoshimura, S. Somiya, Calibration curve for quantitative analysis of the monoclinic-tetragonal ZrO_2 system by X-Ray diffraction, J. Am. Ceram. Soc. 67 (1984) C119–121.
[38] R: A language and environment for statistical computing. R Foundation for Statistical Computing, Vienna, Austria, 2013.
[39] M. Wojdyr, Fityk: a general-purpose peak fitting program, J. Appl. Crystallogr. 43 (2010) 1126–1128.
[40] J.A. Munoz-Tabares, M. Anglada, Quantitative analysis of monoclinic phase in 3Y-TZP by Raman spectroscopy, J. Am. Ceram. Soc. 93 (2010) 1790–1795.

[41] H. Tomaszewski, J. Strzeszewski, L. Adamowicz, V. Sergo, Indirect determination of the piezospectroscopic coefficients of ceria-stabilized tetragonal zirconia polycrystals, J. Am. Ceram. Soc. 85 (2002) 2855–2857.
[42] T. Kosmac, C. Oblak, C. Jevnikar, N. Funduk, L. Marion, The effect of surface grinding and sandblasting on flexural strength and reliability of Y-TZP zirconia ceramic, Dent. Mater. 15 (1999) 426–433.
[43] J.A. Munoz-Tabares, E. Jiménez-Piqué, J. Reyes-Gasga, M. Anglada, Microstructural changes in ground 3Y-TZP and their effect on mechanical properties, Acta Mater. 59 (2011) 6670–6683.
[44] R.H.J. Hannink, M.V. Swain, A mode of deformation in partially stabilized zirconia, J. Mater. Sci. 16 (1981) 1428–1431.
[45] P.E. Reyes-Morel, I.W. Chen, Transformation plasticity of CeO_2-stabilized tetragonal zircona polycrystals: I, Stress assistance and autocatalysis, J. Am. Ceram. Soc. 71 (1988) 343–353.
[46] S. Ban, H. Sato, Y. Suehiro, H. Nakanishi, M. Nawa, Biaxial flexural strength and low temperature degradation of Ce-TZP/Al_2O_3 nanocomposite and Y-TZP as dental restoratives, J. Biomed. Mater. Res. Part B: Appl. Biomater. 87B (2008) 492–498.
[47] M.V. Swain, L.R.F. Rose, Strength limitations of transformation-toughened zirconia alloys, J. Am. Ceram. Soc. 69 (1986) 511–518.
[48] R.M. McMeeking, A.G. Evans, Mechanics of transformation-toughening in brittle materials, J. Am. Ceram. Soc. 65 (1982) 242–246.
[49] A.A. Griffith, The phenomena of rupture and flow in solids, Philos. Trans. R. Soc. London, Ser. A 221 (1921) 163–198.
[50] L. Karygianni, A. Jähnig, S. Schienle, F. Bernsmann, E. Adolfsson, R.J. Kohal, J. Chevalier, E. Hellwig, A. Al-Ahmad, Initial bacterial adhesion on different yttria-stabilized tetragonal zirconia implant surfaces *in vitro*, Materials 6 (2013) 5659–5674.
[51] W. Burger, H.G. Richter, High strength and toughness alumina matrix composites by transformation toughening and "in situ" platelets reinforcement (ZPTA)-The new generation of bioceramics, Key Eng. Mater. 192 (2011) 545–548.